Age and growth rate estimations of the commercially fished gastropod *Buccinum undatum*

Philip R. Hollyman[1]*, Simon R. N. Chenery[2], Melanie J. Leng[3], Vladimir V. Laptikhovsky[4], Charlotte N. Colvin[1] and Christopher A. Richardson[1].

[1]School of Ocean Sciences, College of Natural Sciences, Bangor University, Menai Bridge, Anglesey, LL59 5AB, UK.
[2]Centre for Environmental Geochemistry, British Geological Survey, Nottingham, NG12 5GG, UK
[3]NERC Isotope Geosciences Facilities, British Geological Survey, Nottingham NG12 5GG, UK and Centre for Environmental Geochemistry, School of Biosciences, Sutton Bonington Campus, University of Nottingham, Loughborough, LE12 5RD, UK.
[4]Centre for Environment, Fisheries and Aquaculture Science (CEFAS), Pakefield Road, Lowestoft, Suffolk, NR33 0HT, UK.

*Corresponding author: p.hollyman@bangor.ac.uk

Abstract

Calculating age and growth rate for the commercially important whelk, *Buccinum undatum* in the aid of fishery management has historically been undertaken using growth rings on the organic operculum. This is difficult due to their poor readability and confusion between two different sets of growth lines present. Recent work presented the calcium carbonate statolith as an alternative for age determination of *B. undatum*. Here we compare the use of statoliths and opercula, comparing their readability and creating growth curves for three distinct populations across the UK. Using these data, we also test the most appropriate growth equation to model this species. Lastly, we use oxygen isotope analysis of the shells to assign accurate ages to several individuals from each site. These data were used to test the accuracy of statolith and operculum ages. Statoliths, whilst more time consuming to process have improved clarity and accuracy compared to the opercula. This improved readability has highlighted that a Gompertz growth function should be used for populations of this species, when in past studies, von Bertalanffy is often used. Statoliths are a viable improvement to opercula when assessing *B. undatum* in the context of fishery monitoring and management.

1. Introduction

The common whelk, *Buccinum undatum*, is a cold-water subtidal marine gastropod occurring in the North Atlantic from western shores of Greenland to New Jersey in North America and from Svalbard (Spitzbergen) to France in Europe (FAO, 2018). It is commercially important over much of its range.

The largest fisheries for this species occur in Northern Europe, where the UK leads the production with 22,700 tonnes in 2016 (£22.9 million, MMO, 2017), more than half of the worldwide total of over 41,000 tonnes (FAO, 2018). This fishery has grown drastically since the early 1990s when an increase in export markets saw a rise in both landings and prices (Fahy *et al*., 2005). Concerns are growing over the sustainability of whelk populations in certain areas as there were reports on collapses of some fished populations (Jersey - Shrives *et al*., 2015; Ireland - Fahy *et al*., 2005; North Sea/Netherlands - Ten Hallers-Tjabbes *et al*., 1996) although it has not been confirmed that these declines are necessarily fishery induced (Ten Hallers-Tjabbes *et al*., 1996). This has prompted an increase in research concerning *B. undatum* in recent years covering important topics such regional variation in size at maturity and maturity assessment (Haig *et al*., 2015; McIntyre *et al*., 2015; Borsetti *et al*., 2018; Emmerson *et al*., 2018); fishery based assessments of catches and population structures (Shrives *et al*., 2015; Woods & Jonasson, 2017; Emmerson *et al*., 2018); population genetics (Pálsson *et al*., 2014); mortality estimations (Laptikhovsky *et al*., 2016) and age determination (Hollyman *et al*., 2018a & 2017).

The ability to model stock dynamics is the keystone for all fishery management (Hilborn & Walters, 1992). This requires reliable estimates of growth of the target species and population, to allow the estimation of important parameters such as relating ontogeny to reproductive output and responses to change in fishing pressure (Beamish, 1990; Day & Flemming, 1992; Troynikov *et al*., 1998).

Age determination of molluscs has mostly focussed on bivalves as these contain annually-resolved growth lines visible in sectioned shells (Richardson, 2001) or on the external surface (e.g. *Placopecten magellanicus* [Hart & Chute, 2009]). Annual lines often form as a result of seasonal changes in shell growth rates linked to the availability of food and changes in seawater temperature (see Richardson 2001 for general review). Age determination of gastropods is more difficult as shells which display coiling often cannot be sectioned to reveal the full axis of growth, and *B. undatum* shells do not display external annual growth rings (Gros & Santarelli, 1986; Hollyman, 2017). However, other methods such as operculum and statolith ageing can be used to assess the age of many gastropod species (Hollyman *et al*., 2018b).

1.1 Age estimates based on the operculum

The gastropod operculum is an organic shield like structure found attached to the dorsal side of the foot (Figure 1a). It is used to close off its aperture when the head and foot are retracted, providing protection from both predators and desiccation (Checa & Jiménez-Jiménez, 1998). *B. undatum* display an opercula formed from a protein based secretion from the foot (Hunt, 1969), laid down in concentric rings emanating from a nucleus (Santarelli & Gros, 1985).

Growth rings are present on the dorsal (outer) surface of the operculum of *B. undatum* and have been counted to estimate their age. The rings are thought to form as a result of the periodical slowing of operculum growth during the annual seasonal cycle (Santarelli & Gros, 1985). Secretion of protein layers in the operculum become closer together as growth slows, giving the impression of a distinct band (Figure 1b). Santarelli & Gros (1985) suggested that rings on the operculum surface (OpSR) were annually-deposited and this assumption is widely accepted, although no growth experiments or chemical or isotopic analysis of the opercula were undertaken to confirm it; instead, isotopic analysis of the shell was used as a validating tool for the OpSRs. Their conclusions have been used to apply operculum ageing methods to other populations (e.g. Kideys, 1996; Shelmerdine *et al*., 2007; Heude-Berthelin *et al*., 2011). However, the use of the operculum growth rings is confounded by several common problems such as clarity over different sets of growth lines. A study by Kideys (1996), exemplified this, in a sample of >10,000 whelk opercula, from the Isle of Man, only 16% had clear readable rings and 36% had readable rings that could be used to estimate the age and growth rate of the population. A study from the Centre for Environment, Fisheries and Aquaculture Science (CEFAS) found a similar result: only 13% of opercula were readable (all four readers agreeing) plus 28.3% were of 'conventional agreement' when three of four readers provided the same estimate (Lawler, 2013). Problems arises from the presence of an additional set of growth lines on the ventral (inner) surface of each operculum, known as adventitious layers (OpAL). The growth of the operculum is complex with several areas of growth present on a single operculum (Figure 1d, Checa & Jiménez-Jiménez, 1998, Vasconcelos *et al*., 2012). In a concentric operculum (like those found on *B. undatum*), growth is added to the dorsal (outer) and the structure is also strengthened and thickened over time with the addition of adventitious layers to the ventral side of the operculum (Figure 1c). OpALs on the ventral surface of the operculum appear as clear growth rings (Figure 1c). Possible confusion between OpSRs rings and OpALs could lead to errors in estimating age. Vasconcelos *et al*. (2012) found that neither the OpSRs or OpALs provided a reliable estimation of age for *Hexaplex trunculus*, with the OpALs underestimating and the OpSRs overestimating the age. Although a different species, their work on *H. trunculus* highlights the importance of validating the deposition of growth rings or lines in accreting structures to determine their age. The use of the OpALs as an age estimation tool for *B. undatum* has not previously been validated.

1.2 Age estimates based on the statolith

Statoliths are small (~300µm) calcium carbonate structures found in the nervous system of many gastropod species which are used for gravity perception. Statoliths can contain clear growth rings which represent key life history events such as settlement from the water column (*Tritia* (=*Nassarius*) *reticulatus* [Barroso *et al*., 2005]), hatching from egg capsules (*B. undatum* [Hollyman *et al*., 2018a]) and annual growth rings, representing slowing of growth due to annual temperature cycles (*Neptunea antiqua* [Richardson *et al*., 2005]; *Tritia* (=*Nassarius*) *reticulatus* [Barroso *et al*., 2005; Chatzinikolau & Richardson, 2007]; *Polinices pulchellus* [Richardson *et al*., 2005]). The annual periodicity of statolith growth rings in *B. undatum* has been validated previously using laboratory growth experiments and analysis of shell material (Hollyman *et al*, 2018a) as well as direct chemical analysis of the statoliths (Hollyman *et al*., 2017). It was shown that when statolith rings form in juvenile specimens, a colouration change is also evident, helping to distinguish the annual ring from disturbance rings.

1.3 Age estimates based on oxygen isotope analysis

The oxygen isotope composition of mollusc shells often has a strong relationship with the surrounding seawater temperature at the time of mineralisation (Epstein *et al*., 1953; Leng & Lewis, 2016). Due to this relationship, oxygen isotope ratios (described as $\delta^{18}O$) can be reconstructed at regular intervals over the growth axis of a shell to retrospectively calculate seawater temperature cycles over the life of the animal. In this way, information about not only seawater temperature over time (e.g. *Patella vulgata* [Gutiérrez-Zugasti *et al*., 2017]) but also age and growth rates (e.g. *Conus ermenius* [Sosdian *et al*., 2006]) can be reconstructed. *B. undatum* shells have been analysed in several previous papers as a means of validating growth increments in the operculum (Santarelli & Gros, 1986) and the statolith (Hollyman *et al*., 2018a).

Here we assess the viability of three sets of growth lines found on the accreted structures on *B. undatum* (statolith growth rings [StR], operculum surface rings [OpSR] and adventitious layers [OpAL]) for reconstructing the population age structure and growth rates of wild populations. Alongside this, different models for growth parameter estimation for this species are also investigated to determine the most appropriate. Whilst the classic von Bertalanffy equation had been used in previous studies for this species (e.g. Shelmerdine *et al*., 2007), sigmoidal growth equations such as logistic and Gompertz have been shown to successfully reconstruct the growth of other similar gastropod species (e.g. *Neptunea arthritica* [Miranda *et al*., 2008]). Growth rate data derived from $\delta^{18}O$ of several shells from each sample site are compared to the statolith and operculum derived growth curves to investigate their accuracy. It was hypothesized that the statoliths would produce the most accurate growth curve estimation, whilst displaying the best clarity when compared to both of the operculum derived age estimations, and that a sigmoidal growth equation would best model population growth for this species.

2. Methods

Samples of whelks were collected from three locations across the UK (Shetland, the Menai Strait and Jersey; Figure 2) between February and June 2014 using baited whelk pots soaked for 24 hours. Upon collection, whelks were not sorted (i.e. riddled) and a random sample (of varying amounts depending on site, see Table 1) was collected and frozen at –20°C for later processing.

2.1 Opercula sampling and ageing

Once thawed, the Total Shell Length (TSL) of each whelks was measured to the nearest 0.1 mm using Vernier callipers. Opercula were then removed using forceps, rinsed in freshwater and left to dry overnight at room temperature. Operculum surface rings (OpSR) were counted using transmitted light from either a lamp or a dissecting microscope. Adventitious layers (OpAL) were counted under a dissecting microscope using reflected light as they are more difficult to count without magnification.

2.2 Statolith sampling and ageing

One statolith from each specimen was extracted using the methodology detailed in Hollyman *et al*. (2018a). Once the statoliths had air-dried they were mounted on a microscope slide using Crystalbond™ 509 thermoplastic resin and imaged under a Meiji Techno MT8100 microscope with a Lumenera Infinity 3 microscope camera at 20× magnification. Resulting photomicrographs were then analysed using ImageJ v.1.48 (Ferreira & Rasband 2012), to count and measure the width of each Statolith Ring (StR) from the hatching ring outwards.

2.3 Operculum growth line formation

The timing of operculum growth line formation (OpSR and OpAL) was monitored at the same time as annual StR formation was confirmed during the analysis outlined in Hollyman *et al*. (2018a). Operculum growth line reading was undertaken using the above described methods at regular intervals over the first 2.5 years of life for animals hatched from egg masses (collected from the Menai Strait) and reared in ambient seawater (see Hollyman *et al*. (2018a), for experimental details). The numbers of OpSR and OpAL were then compared with the number of StR from the same specimens.

2.3 Growth ring clarity assessment

The clarity of each of the three sets of growth rings (StR, OpSR and OpAL) was assessed using a modified methodology from Kideys (1996). In order to apply to all 3 sets of growth rings we moved to a 4 tier system.

C1 - No growth rings discernible

C2 - Two or more growth rings unclear

C3 - One growth ring unclear

C4 - All growth rings clear

A comparison of specimens from each of the clarity rankings can be seen in Figure 3. A similar approach to the discarding of unclear specimens was also used with only specimens ranked 3 and 4 in the subsequent analysis. Any samples which were missing were classed as 'not available' (n/a), for statoliths this often constituted the loss of the statolith by the researcher during extraction, for opercula this meant that the sample was lost during potting/collection. This methodology was tested by two of the authors (PRH & CNC) using a random sample of 150 specimens from the Menai Strait for all three sets of growth rings; the results between both readers were then compared.

2.5 Growth curve estimation

Three growth curve equations were fitted to each dataset, using FISHPARM (Prager *et al*., 1994).

Gompertz (1825):

$$L_t = L_0 \, exp^{(G(1-\exp(-gt)))}$$

Where L_t is the mean length at t age (mm), t is age (years), L_0 is the length at t_0 (hatching). G is the instantaneous rate at t_0 and g describes the decrease in the rate of G (Pryzbylski & Garcia-Berthou, 2004). Gg is therefore the specific instantaneous rate of growth at t_0 (Prager *et al*., 1994).

von Bertalanffy (1934):

$$L_t = L_\infty(1 - exp^{-k(t-t0)})$$

Where L_t is the mean length at age t (mm), t is age (years), L_∞ is the asymptotic length (mm), t_0 is the origin of the growth curve and K is considered a stress factor (Moreau & Moreau, 1987; Rodriguez-Sánchez *et al.*, 2009).

Logistic (Verhulst, 1838):

$$L_t = \frac{K}{1 + (\frac{K - L_0}{L_0})\exp(-rt)}$$

Where L_t is the mean length (mm) at age t. L_0 is the mean length at t_0, r is the growth rate and K is the asymptotic length (mm) (Prager *et al.*, 1994).

The von Bertalanffy equation was chosen as it has been used in past studies investigating the growth of *B. undatum* (e.g. Shelmerdine *et al.*, 2007). The logistic and Gompertz equations were chosen as some studies investigating the growth of marine gastropods have found sigmoidal growth (Miranda *et al.*, 2008), which is best modelled by these equations (Windsor, 1932).

The "goodness of fit" of each curve was compared by calculating the R^2 value, the mean squared residual error (MSR_e) and Akaike Information Criterion (AIC), which explicitly penalizes usage of superfluous parameters to achieve a better fit of a particular statistical model (Crawley, 2007). The AIC was calculated using the following equation (Akaike, 1973):

$$AIC = n * ln\left(\frac{SS_{error}}{n}\right) + 2k$$

Where n is the number of observations, SSerror is the sum of squares of the residual of the model output and k is the number of parameters fit within the model. The AIC calculation takes into account both the complexity of the model (i.e. how many parameters are estimated) as well as the residual sum of squares. Once the best fitting model with the least penalized loglikelihood had been chosen, the resulting growth parameters for each site were compared both between sites and between each of the three sets of growth rings within a site.

2.6 Calculation of size for missing age classes

One limiting factor of the data collection was the absence of juvenile specimens from most of the sample sites. A similar problem was also found by Shelmerdine *et al*. (2007) with whelk populations from Shetland and the South coast of England. This resulted in a poor fit for most of the growth curves, for each set of growth rings, as no juvenile data was available to 'pin' the lower estimates for each curve, resulting in unrealistic asymptotic estimates. One option was to force the growth line through 0, this was not appropriate as *B. undatum* enter the water column as fully formed juveniles with a size at t_0 that varies depending on a range of factors, such as egg capsule size and mother size (Nasution *et al*., 2010; Smith & Thatje, 2013). Instead, the typical size at hatching and at 1 year old was modelled for each site by measuring the width of the hatching and 1st annual ring in ImageJ for a random sample of 20 statoliths per site. These measurements were then converted into estimated Total Shell Length (TSL) measurements using the power relationship between statolith width and shell height calculated for combined data from all sites (Hollyman, 2017, pp 183; $R^2 = 0.96$, $n = 1719$):

$$y = 43.439 * x^{0.4259}$$

The reconstructed TSL measurements were then added to the growth curve estimation. As this was not possible for the opercula (due to the poor clarity of early year growth rings) the estimates from the statolith growth rings were also used in the growth curve estimation for both OpSR and OpAL. For the Menai Strait site estimate reliability was improved as, the sizes of the laboratory grown *B. undatum* of known age were used to 'pin' the lower age estimates.

2.7 Oxygen isotope analysis

Shells of three adult male whelks were chosen at each site (plus three females from the Menai Strait), the shells were then cleaned and dried at room temperature. Powder samples were acquired at a set resolution (variable 2 – 4 mm) around the whorls of each shell to reconstruct the $\delta^{18}O$ profile from the entire life history of each specimen, using a Dremel 4000 multitool with a 1mm diamond burr attachment. 50−100 µg of each powder sample was analysed using an Isoprime dual inlet mass spectrometer and Multiprep device at the British Geological Survey (See Hollyman *et al*., 2018a and Hollyman, 2017 for full experimental details). In the context of this paper, the data were not used to reconstruct annual temperature but instead to calculate the annual growth of each animal over its entire life (by calculating the total distance in terms of shell growth between each annual $\delta^{18}O$ cycle). This was done by calculating the relationship between total shell length (TSL) and total lip extension (TLE; i.e. the full coiled 'distance' of growth) for several animals from each site which produced a significant linear relationship (TSL = 0.2421*TLE + 2.7766; R^2 = 0.99; $p < 0.001$). This allowed the conversion of isotope data (taken at a set resolution around the TLE) into TSL values. The annual growths of each specimen were then averaged over each year for each site for a comparison of annual growth rates.

3. Results

3.1 Operculum and statolith growth line formation

Whilst the StRs are clear and unequivocal, the rings on the OpSRs and the OpAls rarely corresponded with the number of statolith rings. The examples shown in Figure 4 are from two 27 month old laboratory reared juvenile *B. undatum* and illustrate the lack of correspondence between the rings in statolith and operculum structures. The statoliths show two annual rings (Figure 4a & d), albeit with several disturbance lines visible. Annual rings are distinguishable from the disturbance lines as they elicit a change in colour, where disturbance rings do not (Hollyman *et al*., 2018a). The corresponding opercula (Figure 4b & c and 4e & f) have many more rings. The OpSRs (Figure 4b & e) have respectively, two and three clear rings with two and one possible (disputed) rings. The OPALs similarly over estimate the number of rings. Figure 4c & f display respectively, four and four rings with an additional possible (disputed) ring in Figure 4e.

In a sample of thirty 27 month old laboratory reared juvenile whelks, 84% displayed two clear statolith rings (the remaining 16% displayed at least two with one or more prominent disturbance rings). By contrast when the corresponding opercula were examined, only 20% displayed two operculum surface rings. Many of the opercula displayed considerable operculum growth after the second ring which likely represents more than 3 months growth (e.g. Figure 4b). Forty percent of opercula had no discernible operculum surface rings and none of the 30 opercula displayed the expected two adventitious layers, with the minimum number of layers being three and the maximum number being six.

3.2 Growth ring clarity assessment

When statoliths and opercula from whelks from all the sites were examined clear differences in the clarity of the growth rings were seen. Figure 5 compares the clarity scores of growth rings from each structure at each site. The statolith rings were clearest at all sites with high percentages scoring 3 and 4 on the clarity scale. The second clearest structure (score 3 & 4) was the OpAL in the opercula with the least clear being the OpSR. Both these structures had a frequency of ≈25% for the clarity score of 1, i.e. no growth rings visible. From a sample of 150 randomly selected statoliths and opercula the agreement in age between two readers was 89.2% agreement for counting the StR, 75.7% agreement in counting the OpAL and 45.1% agreement in counting the OpSR.

3.3 Direct comparison of statolith rings and operculum growth lines

Summary Table 2 presents the average relationships between the ages from each structure at each site (sum of (ageing method 1 / ageing method 2) / *n*). A number >1 indicates an underestimation of age when compared to the statolith rings, values <1 indicate an overestimation of age. All sites except Jersey show an underestimation of age using the operculum surface rings and an overestimation of age using the adventitious layers. The values in Table 2 also display significance (denoted by *) of pairwise comparison t-tests between each set of age data at each site. Interestingly, the comparison of StR and OpSR at Jersey is the only one which was not significantly different.

3.4 Growth curve equation choice

Due to the superior clarity of the growth rings and confidence in their annual periodicity, it was only StR data that was used for growth equation choice. The results displayed in Table 3 show that for the statolith size at age data, for all sites, Gompertz growth curves with the highest R^2 and the lowest MSR_e and AIC values best described the data. For all sites, the Gompertz and logistic equations resulted in a similar goodness of fit, this is unsurprising since both equations model sigmoidal growth (Windsor, 1932), which *B. undatum* seems to display. Therefore for all subsequent analyses the Gompertz growth equation was applied.

3.5 Site growth curve construction

The clarity of the statolith rings was generally good so it was relatively easy to estimate the age of whelks from all the sites and then fit the three growth curves to the size at age data (Table 4). However, the clarity of the OpSRs quickly became an issue when growth curves were initially fitted to all the data. To improve the growth modelling, age estimates based on the OpSRs and OpALs, where there was uncertainty in the data because of the clarity of the rings, were removed. When opercula with a clarity of '1' and '2', were removed from the data, the number of age estimates dropped to unusable levels. To improve this, data where the opercula had a clarity of '2' were again included in order to produce growth curves that could be compared with the statolith growth curves.

The data shown in Figure 6 compare the variance associated with the size at age data and the fitted Gompertz growth curves for the Menai Strait StR, OpSR and OpAL data. The OpSR and OpAL data variance is larger than the variance around the statolith data and reflects the greater accuracy of age estimates using statolith rings. Fitted Gompertz growth curves using both the statolith and opercula generated size at age data for each site are shown in Figure 7, a) using StR, b) using OpSR and c) using

OpAL. For clarity of the growth curves the standard error bars have been omitted in the plots. Using StR data, the whelks from Jersey reached the smallest size whilst the Shetland whelks reached the largest size, which fits with size distribution data. Similar patterns of site specific growth rates was seen in the OpSR and OpAL although the shapes of the sigmoidal curves were different.

Growth curves constructed using the OpSR displayed a steeper rise than those constructed by either the StR or OpAL, with all 3 of the curves demonstrating almost at asymptotic maximum by 6 years of age. This suggests that the OpSRs overestimate the age of each whelk in its early years. Whelks from Jersey had a slow rate of growth after year 2/3 compared to the other populations with the growth rate estimate from the statoliths. None of the plotted growth curves based on the OpAL attained their asymptote by the end of the 10 year period. This suggests that the OpAL likely overestimate the age of the whelks and underestimate annual shell growth. The differences between males and females was investigated for samples from Menai Bridge as this site had the highest sample number, the t0 values are clearly different with males appearing to hatch larger. Later the male whelks appear to attain a greater size (L_∞) than the females. Summary of the calculated growth curve parameters together with the goodness of fit at each site for the three growth structures are shown in Table 4. At every site the StR curves fitted the size at age data generated from the statoliths more closely and with less variability than the OpSR and OpAL data. The calculated L_0 (size at hatching) values also appear to be more realistic using the StR, with most sites ranging between 2.07 mm and 4.85 mm TSL at the time of hatching, which is similar to observed hatchlings. In Table 5, the calculated L_∞ values are compared to the maximum TSL measured in whelks collected from each site. The data show that for all populations the statolith growth rings produced L_∞ values that were closest to the maximum specimen TSL within the sample.

3.6 Oxygen isotope derived age and growth rates

The annual growth rates derived from oxygen isotope analysis (Figure 8a) and the cumulative growth (Figure 8b) highlight the changes in growth rate between the sites over time. The maximum age of each specimen (calculated from these data) were also compared to the number of growth rings in both the statolith and the operculum (Table 6). Overall it shows that the statolith rings have a better reflection of the true age than either of the operculum rings.

4. Discussion and Conclusions

Using a variety of criteria it has been demonstrated that the Statolith rings (StR) provide a more accurate and reliable estimation of age than either the Opercilum Surface Rings (OpSR) or Operculum Adventitious Layers (OpAL). This is likely due to the unreliable formation of operculum growth rings (demonstrated through growth experiments), as well as poor clarity of OpSRs and non-annual formation of OpALs. To our knowledge this is the first study to directly compare operculum, statolith and oxygen isotope ageing techniques to improve age determination of a commercially important gastropod species. The findings of which should result in adoption of StR ageing for fishery assessments of *B. undatum*.

4.1 Clarity of growth rings

The clarity and readability of all 3 sets of growth rings varied between sites, however, the statoliths were the clearest to read at all sites. The statolith growth rings from the juvenile laboratory reared animals were also the clearest when directly compared with the opercula. Two readers were used to assess the number of rings in this part of the research and ages were compared at one site (the Menai Strait), both of the readers (authors PRH & CNC) had extensive experience in mollusc ageing techniques. It is therefore encouraging to find that there was 89.2% agreement between both readers when the StRs were counted, however poor, (45.1%), agreement was achieved in counting the OpSRs.

In the future it is recommended that when statoliths from gastropod populations are investigated, an initial assessment of the accuracy of reading is undertaken routinely so that confidence can be placed in the accuracy of age estimates. It is also highly recommended that for routine use of statolith ageing techniques, multiple readers are used where possible. For this study, the main readers' (PRH) data was checked for consistency regularly (by CNC). The clarity of operculum surface rings from the whelks that were investigated in this study was found to be worse than that in the published literature (41% - 52% readable, Kideys, 1996; Lawler, 2013). Here using the clarity values of '3' and '4', clarity values that were considered to be reasonable to analyse, the reliability ranged between 10 and 40%. In order to provide enough data for constructing growth curves, age estimates from opercula with a clarity of '2' were also included.

4.2 Comparison of statolith and operculum ages

Through direct comparison of the statolith ages with the operculum ages taken from the same animals, it appears that the OpAL consistently overestimate the age of the animal. For Shetland, the Menai Strait and Jersey, an offset linear relationship is seen when compared to the 1:1 lines plotted. The relationships between the OpSRs and StRs appears to change with ontogeny with linear relationships showing underestimation of age in older specimens and overestimation in younger whelks. This could again be linked to the clarity of low age OpSRs discussed earlier. With the knowledge of how adventitious layers are formed, it appears that their function is to thicken and strengthen the operculum over time. If so, then it is unlikely that the adventitious layers would have a clear annual pattern and are simply a weak proxy for increased thickening during periods of shell growth. However, in similar species they do appear to show an annual periodicity e.g. *Coralliophila violacea* (Chen & Soong, 2002), *Buccinum isaotakii* (Ilano *et al*., 2004) and *Neptunea antiqua* (Richardson *et al*., 2005). The oxygen isotope ages (which are reflective of annual changes in seawater temperature, and are assumed here to be the most accurate age determination method) clearly match the StR ages much better than either of the operculum derived ages (Table 6). This adds further support to the more reliable use of StRs.

4.3 Growth modelling

In several previous studies, *B. undatum* growth curves were constructed using OpSR ages, modelled growth using the von Bertalanffy equation (e.g. Hancock, 1963; Santarelli & Gros, 1985; Fahy *et al*., 1995; Kideys, 1996; Shelmerdine *et al*., 2007; Heude-Berthelin *et al*., 2011; Lawler, 2013). In this study, it was apparent that the growth of *B. undatum* is sigmoidal and that the von Bertalanffy equation did not fit the growth data as well as the Gompertz growth equation. Using the Gompertz equation resulted in a growth curve with a much better goodness of fit to the data from all sites. The likely explanation for the difference between previous studies and the current study is a combination of a lack of juvenile whelks from samples coupled with the poor clarity and inaccurate estimates of age from the operculum growth rings. The lack of juvenile whelks is something that was discussed by Shelmerdine *et al*. (2007), who found no whelks < 3 years of age (i.e. no whelks below 30 mm TSL) for sample sites around Shetland. Lawler, (2013) also had minimum sizes of between 20 mm and 30 mm for most of his sampled sites around England and Heude-Berthelin *et al*. (2011), seemingly had no samples below ≈45 mm TSL from west Cotentin, near Jersey. The lack of juvenile (<20 mm) whelks was overcome in the current study by the inclusion of growth data from laboratory reared whelks over the first two years of growth along with the estimation of size at early age classes by back calculating TSL from statolith ring diameter. It is possible that the absence of small size class individuals from many catches represents either a difference in food preference of juvenile whelks (i.e. they are not attracted to the pot bait); this is unlikely as juveniles can be caught in many areas with identical catch methods (Pers. Obs.). Alternatively, this could indicate that juveniles are occupying different habitats to adult whelks, this may be determined by either temperature, food availability and/or predator interactions. This may be indicative of nursery grounds for juvenile whelks that migrate to 'adult' populations at maturity, if so this may represent important management considerations for fisheries. Future work should focus on determining drivers of the presence/absence of juvenile animals from catches to better understand population dynamics.

Only 20% of laboratory reared juveniles displaying the correct age after 27 month, as judged from the operculum. During the course of the research it was observed that OpSR formed during the first few years of growth from field collected adults were the most difficult to read. It is entirely possible that they may be degraded over time as the operculum is composed of organic material which is exposed throughout the life of the animal. The combination of a lack of juveniles and poor clarity of the early age growth rings on the operculum surface likely masked the characteristic initial bend at the lower end of the sigmoidal Gompertz growth curves. The poor clarity of the early growth rings also likely resulted in a proportion of larger incorrectly aged whelks in the lower size classes (i.e. the first one or two annual rings were not counted because they were not visible). This effect can clearly be seen in the growth curves created by Kideys (1996) who had a TSL range of between ≈10 mm and ≈55 mm for whelks that he placed in an age class of 0.5 years. The widest variation in a single age class reported by Kideys was seen at year 3 which spanned from ≈25 mm to ≈120 mm TSL. Although the growth of *B. undatum* does appear to be widely variable within a single population, this finding does seem extreme and unlikely. Subsequent studies have produced more comparable growth curves using OpSR, such as Heude-Berthelin et al. (2011) who sampled *B. undatum* in the West English Channel, close to our samples site of Jersey. The growth curves they produced estimated a size of ~47mm at year two (range 45 – 49) and a size of 55mm at year 4 (range 52 – 60) which were similar to the estimations of our StR curve for Jersey (~40mm and ~60mm for years 2 and 4 respectively).

The choice of the Gompertz growth equation is in line with several other studies that have found sigmoidal growth and fitted Gompertz growth curves to marine gastropod populations (e.g. Troynikov *et al*., 1998 - *Haliotis rubra*; Rodriguez *et al*., 2001 – *Concholepas concholepas*; Chen & Soong, 2002 – *Coralliophila violacea*; Bigatti *et al*., 2007 - *Odontocymbiola magellanica*; Miranda *et al*., 2008 – *Neptunea arthritica*). The annual growth rates derived from oxygen isotope analysis shown in Figure 8a, also support the use of a Gompertz growth curve as all sites show the maximum growth rate in either the second (Menai Strait and Jersey) or third year of growth (Shetland), as opposed to the first year of growth which is characteristic of a von Bertalanffy curve.

4.4 Growth curve comparisons

The StR derived growth curves were shown to have the best goodness of fit in comparison to the OpSR and OpAL derived growth curves from all sites. The OpAL appear to greatly overestimate the age, something that was also seen in the laboratory reared animals, and OpSRs seem to underestimate. The OpSR derived curves displayed faster rates of growth (K) than StR at all sites, however the L_∞ values were lower for all sites. This likely suggests that inaccurately aged whelks are creating an artificial increase in K between one and three years of age for OpSR data and this leads into an under-estimation of L_∞. The underestimated L_∞ is likely due to the difficulty in distinguishing between OpSRs that are compressed together at the edge of the opercula in older whelks. OpSRs are formed from a decrease in the distance between layered organic matter (which forms the growth ring during periods of slow growth), as the growth lines get closer together (through ontogenetic decreases in growth) the ability to differentiate between these layers decreases. Alternatively, whilst the growth rings at the edge of statoliths become closer together, they still appear to be discernible in the oldest statoliths as they are not comprised of stacked layers of organic material but significantly are a continuously forming structure. The values of the growth constant K estimated from the adventitious layers are the lowest at all sites, this is due to the overestimation of age resulting in slow rises in the growth curves.

Differences were also seen between sexes, L_∞ was higher for males which could potentially reflect the repeated greater energy expenditure of females during reproduction over a lifetime (Brokordt *et al*., 2003). The size at hatching (t0) is also greater for males, as this was likely dependent on reconstructed juvenile size classes (from StR measurements) it is unclear whether this difference is genuine, further work determining the sex of newly hatched juveniles should be undertaken to investigate this.

Reported values of L_∞ and K from OpSR in the literature are comparable with those calculated during this study. Shelmerdine *et al*. (2007) calculated values for L_∞ between 99 mm and 157 mm for sites around Shetland, which is comparable with the L_∞ values for the Shetland site found in this study (StR

– 122.2 mm, OpSR – 106.71 mm, OpAL – 105.55 mm). The values of K differed from the values of 0.09 and 0.4 day^{-1} reported by Shelmerdine *et al.*, the StR and OpAL estimations were very close to these values (0.42 and 0.55 day^{-1} respectively) however, the OpSR value was much higher (0.97day^{-1}). The average growth profiles calculated from oxygen isotope data (Figure 8b) also display a sigmoidal growth curve which is most similar to the patterns displayed by the statolith growth rings, rather than either of the operculum growth rings.

There are clear limitations regarding the use of operculum derived age data which likely stem from unreliable formation of growth rings in early years and poor clarity of OpSRs. The growth of OpALs outlined in Figure 1 does not have any clear reason to be annual and is likely representative of strengthening in the operculum. The addition of TSL data from year 0 and year 1, derived from StR measurements represents a novel way of retrospectively adding crucial size data for often missing size classes. Without these data, the Gompertz nature of the growth curves may have been overlooked. Whilst it is conceivable to undertake this practice for the StR data sets (provided the relationship between statolith diameter and TSL for a particular site is known), in this case the year 0 and year 1 statolith data were also included in operculum derived growth curves. Without it, the growth curves for operculum derived ages gave unrealistic estimates of most parameters at all sites. In short, the analysis of the opercula would not have been possible without the use of statolith-derived size at age data and the inclusion of low-clarity operculum specimens. This is more evidence in the preferential use of statoliths in age determination of *B. undatum*. One drawback to the use of statoliths in comparison to opercula is the time taken to extract and process the specimens, 5-10 minutes as opposed to 1-2 minutes. However, the clear advantages to the use of statoliths described here undoubtedly outweigh the collection and processing time.

One issue with the sites from Jersey also needs to be addressed. Many statoliths from the three sample sites displayed extra weaker growth rings between the annual growth lines (Figure 9). The initial inclusion of these extra weak growth rings in age estimations led to an overestimation of the age resulting in values for size at age roughly half of those observed in the Menai Strait population. The Sea Surface Temperature (SST) minima at these two sites are similar, although Jersey reaches higher summer SST values; this finding was a clear anomaly that led to further investigation of the weaker growth rings. Their formation is likely due to a slowing of growth during the summer maximum temperatures at this site. The extra lines were more of an issue in samples from Jersey which has higher maximum annual SST that the other two sites and is nearby of the southern limit of the species range so its thermal tolerance of summer temperatures. This suggests that *B. undatum* has an optimum growth temperature range, and that whelks in Jersey may experience deviations from both the optimal temperature minima and maxima during the annual cycle. With practice it is simple to discount these extra lines, which often do not remain clearly visible as disturbance lines around the whole circumference of the statolith (Figure 9). This issue raises the importance of fully understanding the environmental setting of locations from which whelk samples are collected to better aid in the interpretation of their statolith rings.

In conclusion, the statoliths of *B. undatum* provide a more reliable method of age estimation than the currently used operculum surface rings. The statolith rings are superior in both their clarity and the variability of the resulting growth curves. The growth of *B. undatum* was shown for the first time to follow a sigmoidal development that is most accurately modelled using a Gompertz growth function. With further refinement and observation the statolith ageing techniques presented here hold great promise for improving the feasibility of stock and population structure assessments for the currently difficult to assess yet commercially important *B. undatum* populations around the U.K and from European waters.

Acknowledgements

This project funded by a Bangor University-CEFAS PhD scholarship awarded to PRH. The authors would like to thank Gwyne Parry-Jones (School of Ocean Sciences, (SOS), Bangor University), Mark Hamilton (NAFC) and Jon Shrives (DoE Jersey) for all their help in sample collection. Thanks also to Berwyn Roberts who helped maintain juvenile whelks in the aquarium. All stable isotope sampling was undertaken following a successful facility grant application to the NERC Isotope Geoscience Facility Steering Committee (NIGFSC) (IP−1527−0515), for which we thank Hilary Sloane processing the samples. We also thank Dr. Alexander Arkhipkin and three anonymous reviewers for their comments and editorial feedback which greatly improved the paper.

References

Akaike, H. 1973. Information theory and an extension of the maximum likelihood principle. *In* 2nd International Symposium on Information Theory. Ed. By B. N. Petrov, F. Csáki. Tsahkadsor, Armenia, USSR, September 2-8, 1971, Budapest: Akadémiai Kiadó. 451 pp.

Beamish, R. J. 1990. The importance of accurate ages in fisheries sciences. *In* The Measurement of Age and Growth in Fish and Shellfish. Ed. By D. A. Hancock. Proceedings No. 12. Bureau of Rural Resources, Canberra, Australia. 320 pp.

Bertalanffy V, L. 1938. A quantitative theory of organic growth. Human Biology, 10(2): 181-213.

Barroso, C. M., Nunes, M., Richardson, C.A., and Moreira, M.H. 2005. The gastropod statolith: a tool for determining the age of *Nassarius reticulatus*. Marine Biology, 146: 1139–1144.

Bigatti, G., Penchaszadeh, P. E., and Cledón, M. 2007. Age and growth in *Odontocymbiola magellanica* (Gastropoda: Volutidae) from Golfo Nuevo, Patagonia, Argentina. Marine Biology, 150: 1199-1204.

Borsetti, S., Munroe, D., Rudders, D. B., Dobson, C., and Bochenek, E. A. 2018. Spatial variation in life history characteristics of waved whelk (*Buccinum undatum* L.) on the U.S. Mid-Atlantic continental shelf. Fisheries Research, 198: 129-137.

Brokordt, K., Guderley, H., Guay, M., Gaymer, C. F., Himmelman, J. H. 2003. Sex differences in reproductive investment: maternal care reduces escape response capacity in the whelk *Buccinum undatum*. Journal of Experimental Marine Biology and Ecology, 291: 161-180

Chatzinikolaou, E., and Richardson, C. A. 2007. Evaluating growth and age of netted whelk *Nassarius reticulatus* (Gastropoda: Nassariidae) using statolith growth rings. Marine Ecology Progress Series, 342: 163-176.

Checa, A. G., and Jiménez-Jiménez, A. P. 1998. Constructional Morphology, Origin, and Evolution of the Gastropod Operculum. Paleobiology, 24(1): 109-132.

Chen, M. H., and Soong, K. 2002. Estimation of age in the sex-changing, coral-inhabiting snail *Coralliophila violacea* from the growth striae on the opercula and a mark-recapture experiment. Marine Biology, 140: 337-342.

Crawley, M. J. 2007. The R book. John Wiley & Sons Ltd, Chichester, U.K. 942 pp.

Day, R. W., and Fleming, A. E. 1992. The determinants and measurement of abalone growth. pp. 141-168. *In* Abalone of the World: Biology. Fisheries, and Culture. Ed. By Shepherd, S. A., Tegner, M. J., and Guzmin del Prao, S. A. Fishing News Books, Oxford, UK. 608 pp.

Emmerson, J. A., Haig, J. A., Bloor, I. S. M., and Kaiser, M. J. 2018. The complexities and challenges of conserving common whelk (*Buccinum undatum* L.) fishery resources: Spatio-temporal study of variable population demographics within an environmental context. Fisheries Research, 204: 125-136.

Epstein, S., Buchsbaum, J. R., Lowenstam, H. A. & Urey, H. C. 1953. Revised carbonate-water isotopic temperature scale. Geological Society of America Bulletin, 64: 1315-1326.

Fahy, E., Yalloway, G., and Gleeson, P. 1995. Appraisal of the whelk *Buccinum undatum* fishery of the Southern Irish Sea with proposals for a management strategy. Irish Fisheries Investigations Series B, 42.

Fahy E, Carroll J, O'Toole M, Barry C, Hother-Parkes L (2005) Fishery associated changes in the whelk *Buccinum undatum* stock in the southwest Irish Sea, 1995-2003. Irish Fisheries Investigations, 15.

Food and Agriculture Organization species distribution maps. http://www.fao.org/figis/geoserver/factsheets/species.html

Ferreira, T., and Rasband, W. 2012. ImageJ User Guide 1.46r. ImageJ/Fiji. 198 pp.

Gompertz, B. 1825. On the Nature of the Function Expressive of the Law of Human Mortality, and on a New Method of Determining the Value of Life Contingencies. Philosophical Transactions of the Royal Society, 115: 513-585.

Gros, P., and Santarelli, L. 1986. Methode d'estimation de la surface de pêche d'un casier á l'aide d'une filiere experimentale. Oceanologica Acta, 9: 81-87.

Gutiérrez-Zugasti, I., Suárez-Revilla, R., Clarke, L. J., Schöne, B. R., Bailey, G. N., and González-Morales, M. R. 2017. Shell oxygen isotope values and sclerochronology of the limpet *Patella vulgata* Linnaeus 1758 from northern Iberia: Implications for the reconstruction of past seawater temperatures. Palaeogeography, Palaeoclimatology, Palaeoecology, 475: 162-175.

Haig, J. A., Pantin, J. R., Murray, L. G., and Kaiser, M. J. 2015. Temporal and spatial variation in size at maturity of the common whelk (*Buccinum undatum*). ICES Journal of Marine Science, 72 (9): 2707-2719.

Hancock, D. A. 1963. Marking experiments with the commercial whelk (*Buccinum undatum*). ICNAF Special Publication, 4:176-187.

Hart, D. R., and Chute, A. S. 2009. Verification of Atlantic sea scallop (*Placopecten magellanicus*) shell growth rings by tracking cohorts in fishery closed areas. Canadian Journal of Fisheries and Aquatic Sciences, 66: 751-758.

Heude-Berthelin, C., Hégron-Macé, L., Legrand, V., Jouaux, A., Adeline, B., Mathieu, M., and Kellner, K. 2011. Growth and reproduction of the common whelk *Buccinum undatum* in west Cotentin (Channel), France. Aquatic living resources, 24: 317–327.

Hilborn, R., and Walters, C. J. 1992. Quantitative fisheries stock assessment: choices, dynamics and uncertainty. New York: Chapman and Hall. Chicago. 570 pp.

Hollyman, P. R., Leng, M. J., Chenery, S. R. N., Laptikhovsky, V. V., and Richardson, C. A. 2018a. Statoliths of the whelk *Buccinum undatum*: a novel age determination tool. Marine Ecology Progress Series, 598: 261–272. doi: 10.3354/meps12119.

Hollyman, P. R., Chenery, S. R. N., EIMF, Ignatyev, K., Laptikhovsky, V. V., and Richardson, C. A. 2017. Micro-scale geochemical and crystallographic analysis of *Buccinum undatum* statoliths reveals annual periodicity of visible growth rings. In Press, Chemical Geology, doi.org/10.1016/j.chemgeo.2017.09.034

Hollyman, P. R., Laptikhovsky, V. V., and Richardson, C. A. 2018b. Techniques for estimating the growth of molluscs. I: Gastropods. In press: Journal of Shellfish Research.

Hollyman, P. R. 2017. Age, growth and reproductive assessment of the whelk, *Buccinum undatum*, in coastal shelf seas. PhD thesis, Bangor University. 404 pp. http://e.bangor.ac.uk/9872/

Hunt, S. 1969 Characterization of the operculum of the gastropod mollusc *Buccinum undatum.* Biochimica et Biophysica Acta, 207: 347-360.

Ilano, A. S., Fujinaga, K., and Nakao, S. J. 2004. Reproductive cycle and size at sexual maturity of the commercial whelk *Buccinum isaotakii* in Funka Bay, Hokkaido, Japan. Journal of the Marine Biological Association of the United Kingdom, 83: 1287–1294.

Kideys, A. E. 1996. Determination of age and growth of *Buccinum undatum* L. (Gastropoda) off Douglas, Isle of Man. Helgoländer Meeresuntersuchungen, 50: 353–368.

Laptikhovsky, V., Barrett, C., Firmin, C., Hollyman, P., Lawler, A., Masefield, R., McIntyre, R., Palmer, D., Soeffker, M., Parker-Humphreys, M. 2016. A novel approach for estimation of the natural mortality of the common whelk, *Buccinum undatum* (L.) and role of hermit crabs in its shell turnover. Fisheries Research, 183: 146-154.

Lawler, A. 2013. Determination of the size of maturity of the whelk *Buccinum undatum* in English waters − Defra Project MF0231. 39 pp.

Leng, M. J., & Lewis, J. P. 2016. Oxygen isotopes in Molluscan shell: Applications in environmental archaeology. Environmental Archaeology, 21(3): 295-306.

McIntyre, R., Lawler, A., and Masefield, R. 2015. Size of maturity of the common whelk, *Buccinum undatum*: Is the minimum landing size in England too low? Fisheries Research, 162: 53–57.

Miranda, R. M., Fujinaga, K., and Nakao, S. 2008. Age and growth of *Neptunea arthritica* estimated from growth marks in the operculum. Marine Biology Research, 4: 224-235.

Marine Management Organisation. 2017. UK Sea Fisheries Statistics 2016. Office for National Statistics, London, UK. 174 pp.

Moreau, J. and Moreau, I. 1987. Fitting of von Bertalanffy growth function (VBGF) with two growth checks per year. Journal of Applied Ichthyology, 3: 56-60. doi:10.1111/j.1439-0426.1987.tb00453.x

Nasution, S., Roberts, D., Farnsworth, K., Parker, G. A., and Elwood, R. W. 2010. Maternal effects on offspring size and packaging constraints in the whelk. Journal of Zoology, 281: 112-117.

Pálsson, S., Magnúsdóttir, H., Reynisdóttir, S., Jónsson, Z., and Ornólfsdóttir, E. B. 2014. Divergence and molecular variation in common whelk *Buccinum undatum* (Gastropoda: Buccinidae) in Iceland: a trans-Atlantic comparison. Biological Journal of the Linnean Society, 111: 145–159.

Prager, M. H., Saila, S. B., and Recksiek, C. W. 1994. FISHPARM: A microcomputer program for parameter estimation of non-linear Models in fishery science. Old Dominion University Oceanography Technical Report 87–10. 22 pp.

Przybylski, M., and García-Berthou, E. 2004. Age and growth of European bitterling (*Rhodeus sericeus*) in the Wieprz-Krzna Canal, Poland. Ecohydrology & Hydrobiology, 4(2): 207–213.

Richardson, C. A. 2001. Molluscs as archives of environmental change. Oceanography and Marine Biology: an Annual Review, 39: 103–164.

Richardson, C. A., Saurel, C., Barroso, C. M., and Thain, J. 2005. Evaluation of the age of the red whelk *Neptunea antiqua* using statoliths, opercula and element ratios in the shell. Journal of Experimental Marine Biology and Ecology, 325: 55–64.

Rodriguez, L., Daneri, G., Torres, C., León, M., and Bravo, L. 2001. Modeling the growth of the Chilean loco, *Concholepas concholepas* (Bruguiere, 1789) using a modified Gompertz-type function. Journal of Shellfish Research, 20: 309–315.

Rodriguez-Sánchez, V., Encina, L., Rodríguez-Ruiz, A., and Sánchez-Carmona, R. 2009. Largemouth bass, *Micropterus salmoides*, growth and reproduction in Primera de Palos' lake (Huelva, Spain). Folia Zoologica, 58(4): 436-446.

Santarelli, L., and Gros, P. 1985. Age and growth of the whelk *Buccinum undatum* L. (Gastropoda: Prosobranchia) using stable isotopes of the shell and operculum striae. Oceanologica Acta, 8: 221–229.

Shelmerdine, R. L., Adamson, J., Laurenson, C. H., and Leslie, B. 2007. Size variation of the common whelk, *Buccinum undatum*, over large and small spatial scales: Potential implications for micro-management within the fishery. Fisheries Research, 86: 201-206.

Shrives, J. P., Pickup, S. E., and Morel, G. M. 2015. Whelk (*Buccinum undatum* L.) stocks around the Island of Jersey, Channel Islands: Reassessment and implications for sustainable management. Fisheries Research, 167: 236–242.

Smith, K. E., and Thatje, S. 2013. Nurse egg consumption and intracapsular development in the common whelk *Buccinum undatum* (Linnaeus 1758). Helgoland Marine Research, 67: 109-120.

Ten Hallers-Tjabbes, C. C., Everaarts, J. M., Mensink, B. P., and Boon, J. P. 1996. The decline of the North Sea whelk (*Buccinum undatum* L.) between 1970 and 1990: a natural or human-induced event? Marine Ecology, 17: 333–343.

Sosdian, S., Gentry, D. K., Lear, C. H., Grossman, E. L., Hicks, D., and Rosenthal, Y. 2006. Strontium to calcium ratios in the marine gastropod *Conus ermineus*: growth rate effects and temperature calibration. Geochemistry Geophysics Geosystems, 7(11): 1525-2027.

Troynikov, V. S., Day, R. W., and Leorke, A. M. 1998. Estimation of seasonal growth parameters using a stochastic Gompertz model for tagging data. Journal of Shellfish Research, 17(3): 833-838.

Vasconcelos, P., Gharsallah, I. H., Moura, P., Zamouri-Langar, L., Gaamour, A., and Missaoui, H. 2012. Appraisal of the usefulness of operculum growth marks for ageing *Hexaplex trunculus* (Gastropoda: Muricidae): Comparison between surface striae and adventitious layers. Marine Biology Research, 8: 141-53.

Verhulst, P. F. 1838. Notice sur la loi que la population suit dans son accroissement. Current Maths and Physics, 10: 113.

Vovelle, J. 1967. Sur l’opercule de *Gibbula magus* L. gastéropode Prosobranch: édification, nature proteique et durcissement par tannage quinonique. Comptes rendus de l'Académie des Sciences, 264: 141-144.

Windsor, C. P. 1932. The Gompertz curve as a growth curve. PNAS, 18(1): 1-8.

Woods, P., and Jonasson, J. P. 2017. Bayesian hierarchical surplus production model of the common whelk Buccinum undatum in Icelandic waters. Fisheries Research, 194: 117-128.

Figure legends

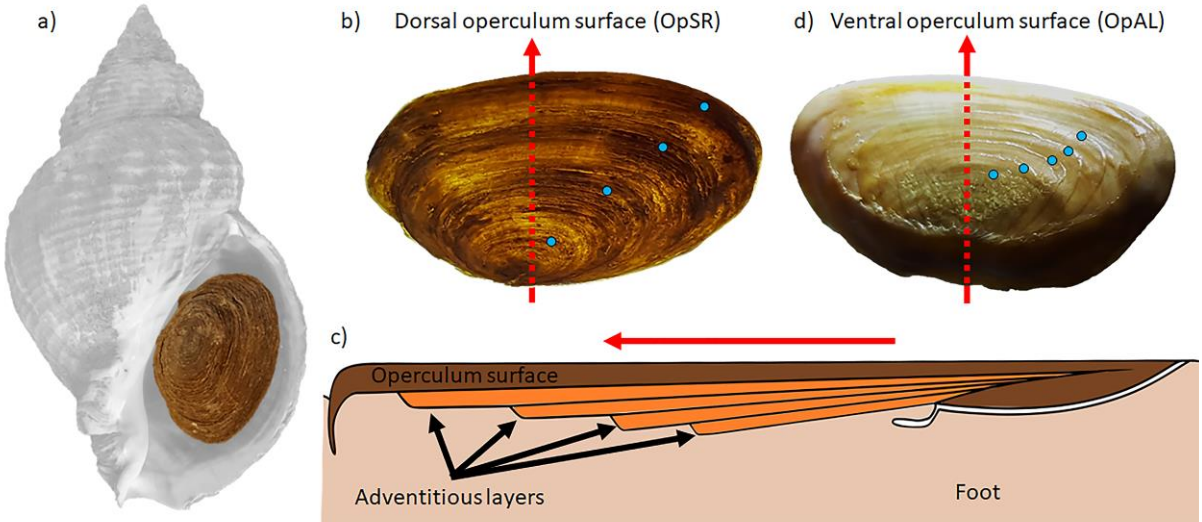

Figure 1. a) the location of the operculum on a whole whelk highlighting the exposed dorsal surface, b) a view of the operculum dorsal surface, c) a view of the operculum ventral surface, growth rings are highlighted with blue dots. d) a diagrammatic representation of the growth of the concentric operculum of *B. undatum*. Red lines indicate the direction of growth. Adapted from Vovelle, (1967) and Checa and Jiménez-Jiménez (1998).

Figure 2. The localities of all three sampling sites used in this study.

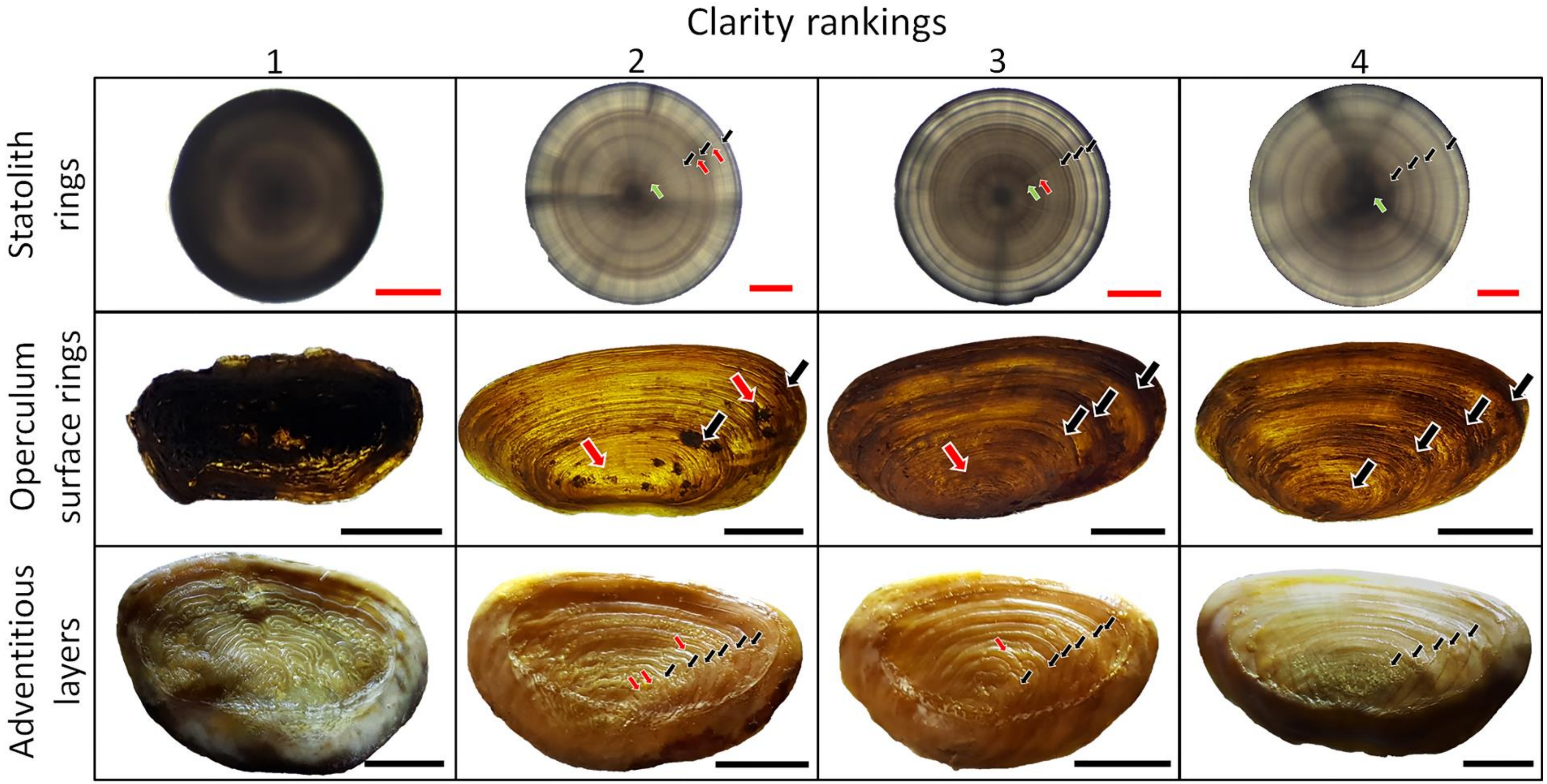

Figure 3. *Buccinum undatum* statoliths and opercula. A comparison of four levels of clarity of StR (top row), OpSR viewed in transmitted light (middle row) and OpAL viewed in reflected light (bottom row). Red lines indicate 50 µm scale bars, black lines represent 5 mm scale bars. Black arrows represent clear growth lines, red arrows represent unclear growth lines and green arrows represent the hatching ring of the statoliths

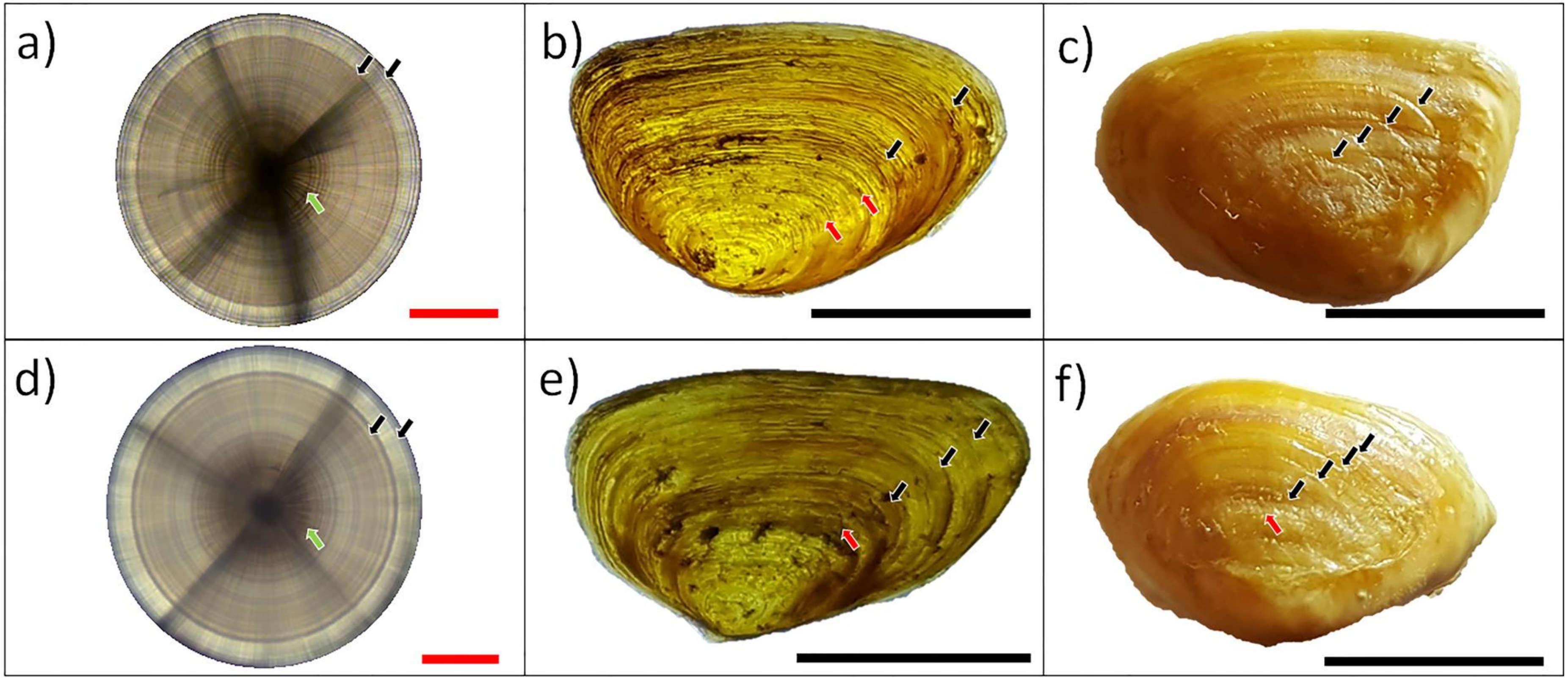

Figure 4. Photomicrographs of two 27 month old laboratory reared *Buccinum undatum* statoliths (a & d) with corresponding operculum, external surface (b & e) and operculum inner surface showing the adventitious layers (c & f). Hatching rings are represented by green arrows (a & d), clear growth rings by black arrows and disputed rings by red arrows. The statolith rings and operculum surface rings (a & d and b & e respectively) were imaged with transmitted light whereas the adventitious layers on the inner surface of each operculum (c & f) were imaged using reflected light. Red lines indicate 50 µm scale bars, black lines represent 5 mm scale bars.

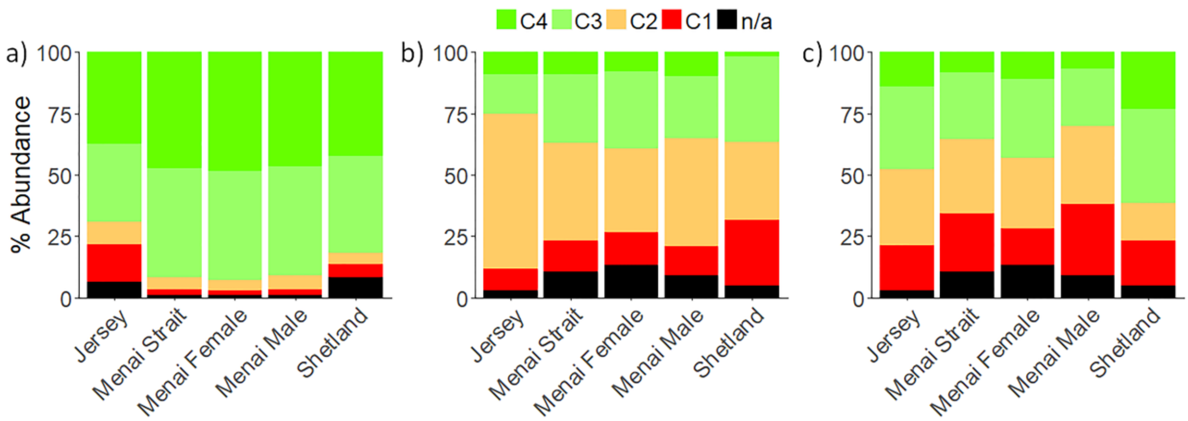

Figure 5. Comparison of stacked bar plots showing the % frequency of clarity scores (C4 is best) for a) statoliths, b) operculum surface rings and c) adventitious layers from *Buccinum undatum* collected from all sites. n/a represents samples where one or more structures were lost or were not collected during sampling processing.

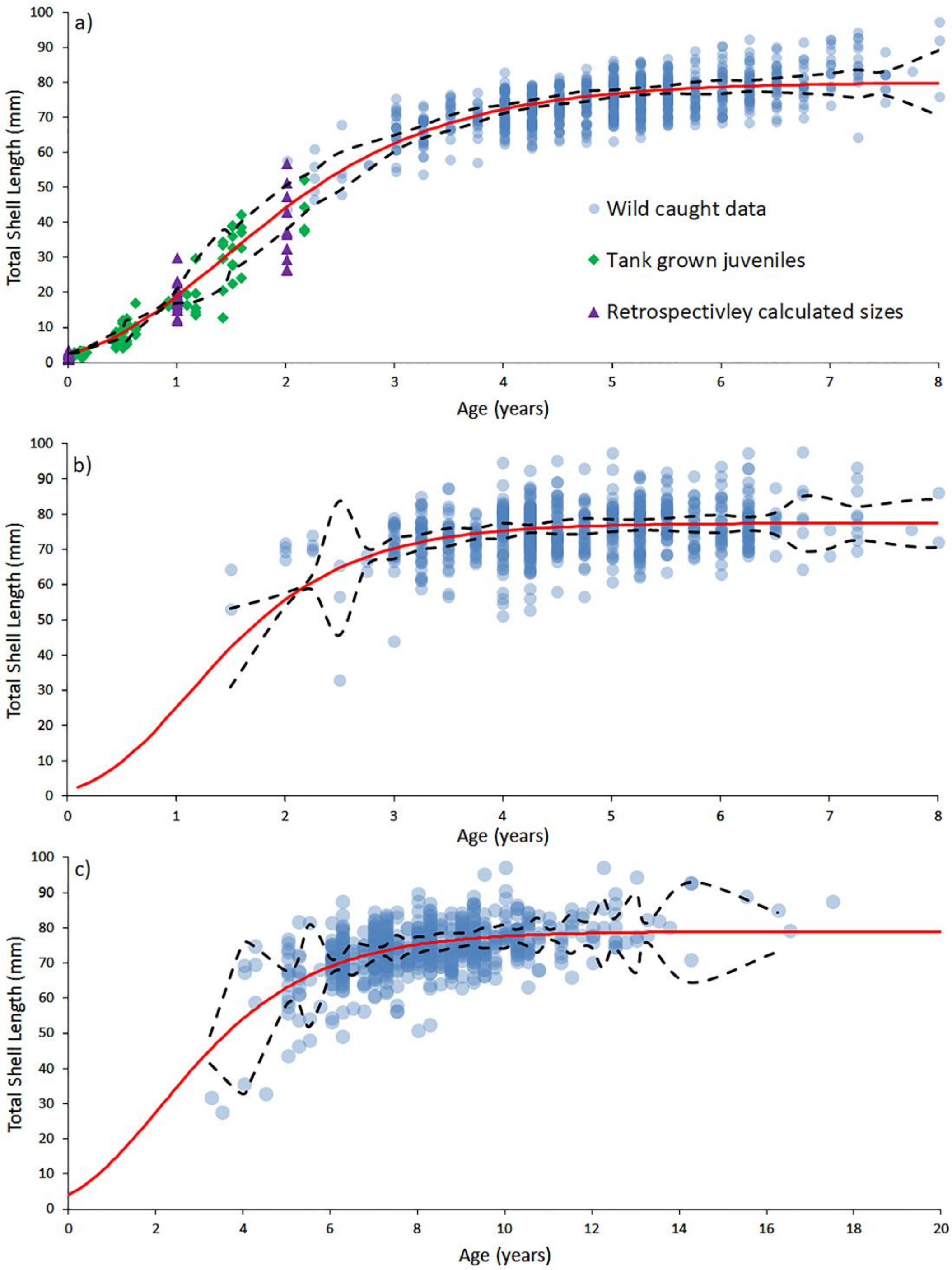

Figure 6. Gompertz growth curves for *Buccinum undatum* from the Menai Strait (red lines) for (a) statolith ring data, (b) operculum surface rings and (c) adventitious layers. Note that the x-axis for graph c) is almost twice the size of a) and b) due to the high age estimations of adventitious layers. Dotted lines represent 95% confidence intervals. Blue dots represent data from wild caught animals, green diamonds represent aquarium growth data, purple trianglesrepresent retrospectively calculated size at age from statoliths rings.

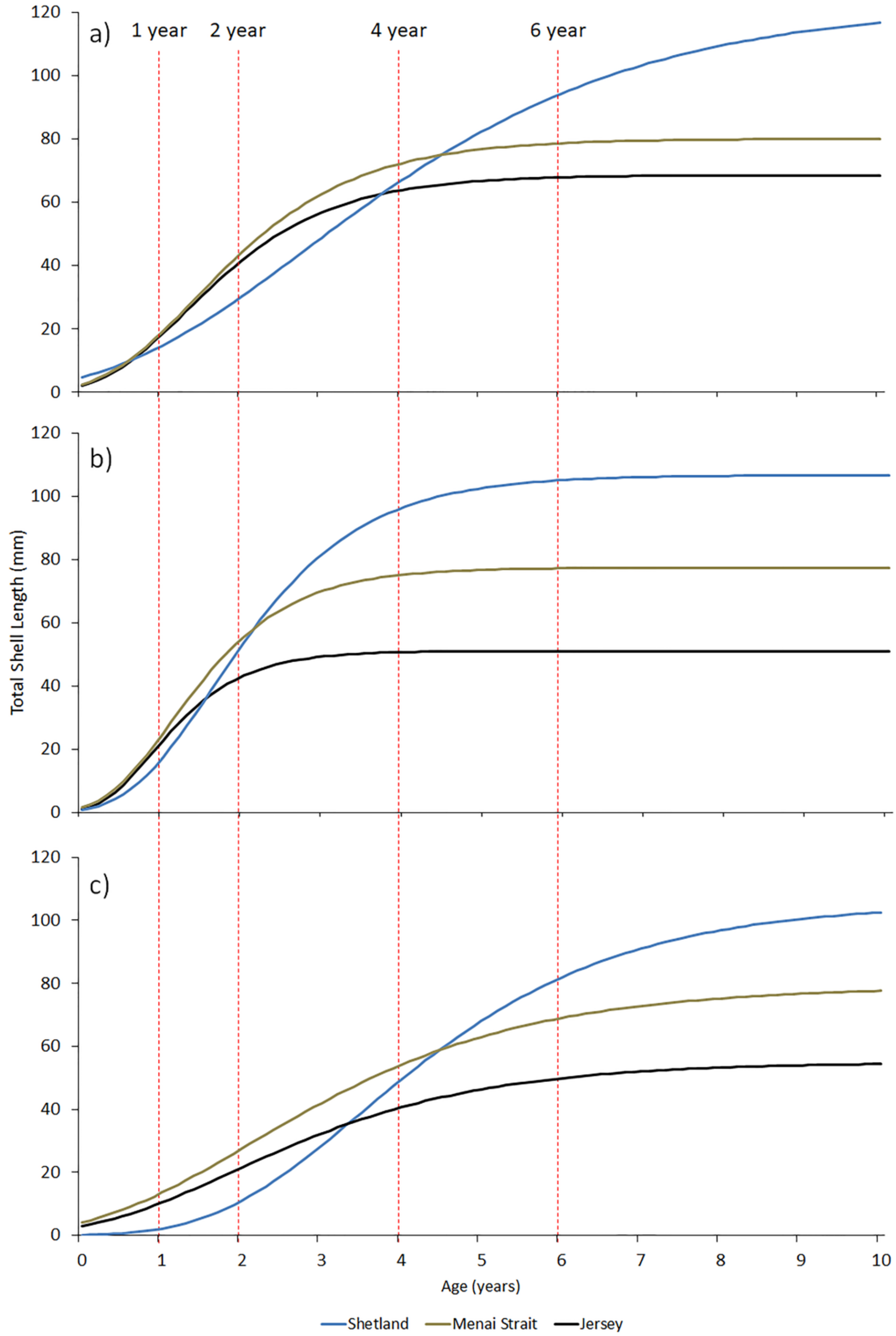

Figure 7. Fitted Gompertz growth curves for *Buccinum undatum* from the Shetland Isles (blue lines), the Menai Strait (brown lines), Jersey (black lines). The data in a) were fitted using data generated from statolith rings, the data in b) were fitted using operculum surface rings and the data in c) were fitted using adventitious layers. Vertical dotted red lines represent 1, 2, 4 and 6 year marks.

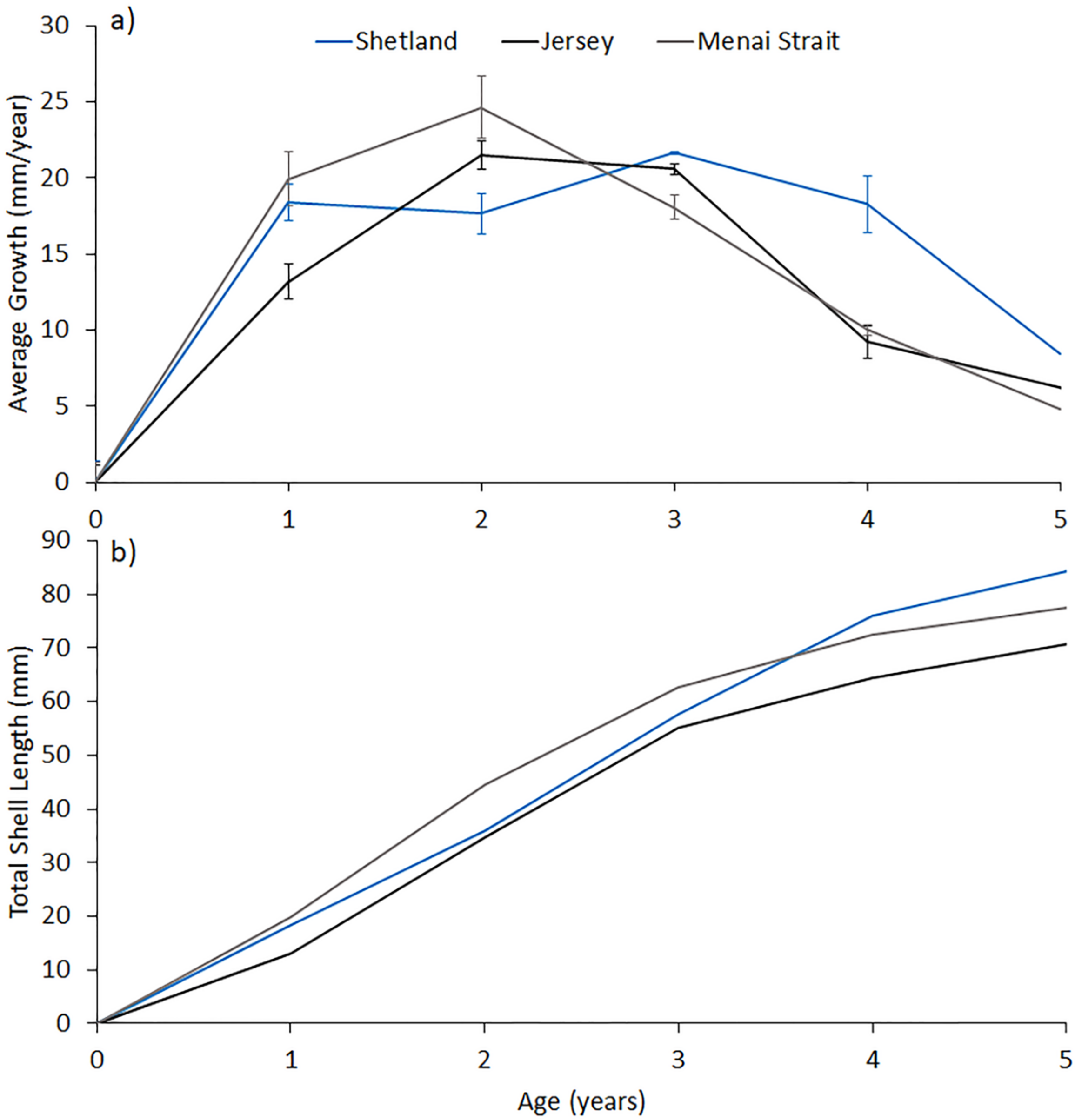

Figure 8. a) Annual growth rates of individual field collected whelks from Jersey, the Menai Strait and Shetland whelks. Average profiles are shown from all sampled shells from each site, error bars represent +/– 1SE. b) Average cumulative growth over time, derived from isotope growth rate data.

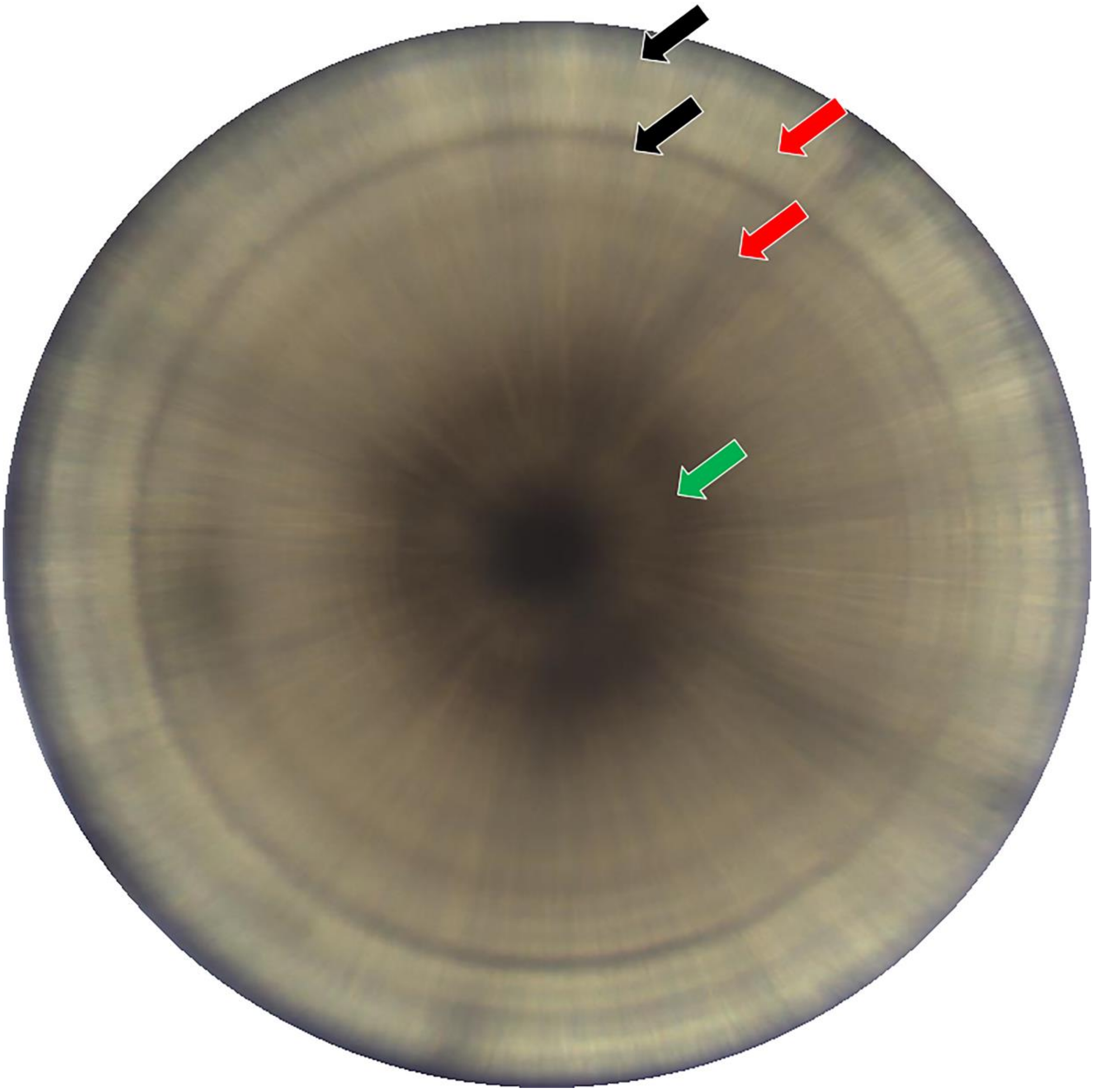

Figure 9. A *Buccinum undatum* statolith from a 2 year old male specimen from JD5. The hatching and annual growth rings are clearly visible (green and black arrows respectively). The weaker mid-annual lines are shown with red arrows.

Tables

Table 1. The locations, date of collection, depth and number of samples from each sample site.

Site name	Latitude	Longitude	Date	Depth (m)	Number of whelks
Menai Strait	53.2338889	-4.143055556	Feb '14 - Jul '15	10 - 11.5	50/month (900)
Jersey	49.193889	-1.858611	Feb '15	14	91
Shetland	60.64333	-0.969444	Feb '15	18 - 20	218

Table 2. The average differences between corresponding statolith ring ages and operculum derived ages for each site. Values >1 indicate an underestimation of age, values <1 indicate an overestimation of age. * denotes a p value < 0.001 for pairwise comparison t tests between groups.

	OpSR vs. StR	OpAL vs. StR	OpSR vs. OpAL
Shetland	1.31*	0.66*	0.40*
Menai Strait	1.03*	0.54*	0.54*
Jersey	0.89	0.40 *	0.45*

Table 3. Goodness of fit indicators for the three growth models (Gompertz, von Bertalanffy and Logistic) applied to the statolith growth ring size at age data from each site. Bold text indicates the best fitting model for each site.

Model	Parameter	Jersey	Menai Strait (All)	Menai Strait Female	Menai Strait Male	Shetland
Gompertz	R^2	**0.90**	**0.94**	**0.97**	**0.97**	**0.99**
	MSR_e	**26.9**	**27.1**	**28.9**	**25.9**	**20.7**
	AIC	**3.30**	**3.30**	**3.37**	**3.26**	**3.05**
Von Bertalanffy	R^2	0.88	0.93	0.95	0.96	0.98
	MSR_e	30.0	31.1	38.2	29.8	24.9
	AIC	3.42	3.44	3.65	3.4	3.24
Logistic	R^2	0.89	0.94	0.96	0.96	0.98
	MSR_e	27.8	29.4	30.4	29.3	24.7
	AIC	3.34	3.38	3.42	3.38	3.23

Table 4. Parameter outputs and goodness of fit indicators from Gompertz growth curves fitted to size at age data generated using StR data (top table), OpSR data (middle table) and OpAL data (bottom table) for all sites. Bold text indicates the best fitting model at each site.

Statolith Rings

	Jersey	Menai Strait	Menai Strait female	Menai Strait male	Shetland

L0 (mm)	2.07 ±0.55	2.45 ±0.33	2.35 ±0.29	3.31 ±0.3	4.85 ±0.56
L_∞ (mm)	68.57	80.04	79.14	83.57	122.2
K	0.97 ±0.06	0.88 ±0.02	0.87 ±0.02	0.74 ±0.01	0.55 ±0.02
R^2	**0.89**	**0.94**	**0.97**	**0.97**	**0.98**
MSR_e	**26.90**	**27.18**	**28.88**	**25.90**	**20.67**
n	217	871	398	473	153
			Operculum surface rings		
	Jersey	Menai Strait	Menai Strait female	Menai Strait male	Shetland
L0 (mm)	1.02 ±0.81	1.66 ±0.41	0.51 ±0.25	1.59 ±0.38	0.9 ±0.59
L_∞ (mm)	51.10	77.45	75.43	79.34	106.71
K	1.58 ±0.2	1.22 ±0.05	1.37 ±0.09	1.07 ±0.04	0.97 ±0.08
R^2	0.72	0.89	0.94	0.94	0.91
MSR_e	69.17	52.50	51.44	44.82	131.14
n	244	646	251	395	121
			Adventitious layers		
	Jersey	Menai Strait	Menai Strait female	Menai Strait male	Shetland
L0 (mm)	2.92 ±1.65	4.15 ±0.52	3.33 ±0.45	4.33 ±0.56	0.13 ±0.29
L_∞ (mm)	54.92	78.79	75.38	79.73	105.55
K	0.57 ±0.08	0.51 ±0.02	0.66 ±0.04	0.49 ±0.02	0.42 ±0.08
R^2	0.71	0.92	0.97	0.95	0.89
MSR_e	66.19	40.30	26.60	38.15	122.83
n	218	553	245	308	136

Table 5. Summary of the Total Shell Length (TSL) data for each site along with a comparison between the maximum TSL values and the L_∞ value produced by the Gompertz equation using each of the 3 structures at each site. Bold text indicates the best fit at each site. Maximum differences were calculated by subtracting the maximum Total Shell Length (TSL) measurement at each site from the L_∞ calculated at each site.

TSL (mm)	Jersey	Menai Strait	Menai Strait female	Menai Strait male	Shetland
Mean	44.40	75.05	74.00	75.98	92.26

Max.	70.56	97.87	97.51	97.87	115.30
Min.	22.84	27.82	34.74	27.82	44.25
Maximum difference from L_∞ (statolith rings)	**1.99**	**17.83**	**18.37**	**14.30**	**-6.90**
Maximum difference from L_∞ (operculum surface rings)	19.46	20.42	22.08	18.53	8.59
Maximum difference from L_∞ (adventitious layers)	15.64	19.08	22.13	18.14	9.75

Table 6. Comparison of age and shell isotope data for all sampled specimens. Grey boxes denote a miss-match between the highlighted value and the number of shell oxygen isotope cycles. * indicate that the statolith sample contained 1 or more disturbance rings. ? indicate where an operculum has poor clarity.

Location	Sample	No. of $\delta^{18}O$ cycles in shell	No. of statolith rings	No. of operculum surface rings
Laboratory reared animals	T1	2	2	0
	T2	2	2	3
	T3	2	2	2
Menai Strait Female	Pilot shell	3	3	4
	MS13-7	3	3*	2?
	MS13-23	4	4	3?
Menai Strait Male	MS13-3	5	5*	3
	MS13-13	4	4	2?
	MS13-33	4	4	4
Jersey Male	JF4-4	5	5*	4?
	JF4-5	5	5*	4
	JF4-9	5	5*	3?
Shetland Male	SH-19	6	6	3?
	SH-31	5	5	3?
	SH-32	5	5	4?